Compact and Wideband Microstrip Bandstop Filter

Ming-Yu Hsieh and Shih-Ming Wang

***Abstract*—A novel one-section bandstop filter (BSF), which possesses the characteristics of compact size, wide bandwidth, and low insertion loss is proposed and fabricated. This bandstop filter was constructed by using single quarter-wavelength resonator with one section of anti-coupled lines with short circuits at one end. The attenuation-poles characteristics of this type of bandstop filters are investigated through TEM transmission-line model. Design procedures are clearly presented. The 3-dB bandwidth of the first stopband and insertion loss of the first passband of this BSF is from 2.3 GHz to 9.5 GHz and below 0.3 dB, respectively. There is good agreement between the simulated and experimental results.**

***Index Terms*—Bandstop filter (BSF), microstrip, quarter-wavelength resonator, transmission zero.**

I. Introduction

BANDSTOP filter (BSF) is one of the key building blocks in modern communication system. It plays a major role of filtering out the unwanted signals and passing the desired signal. Active devices, such as oscillator and mixer, are often followed by BSFs to remove the higher order harmonics and other unwanted spurious signals, respectively. Moreover, numerous microwave components including of diplexers and switches are also comprised of BSF.

Microstrip-line BSFs have the advantages of low-cost, low-weight, and ease of implementation. Conventional microstrip BSF [1] is composed of shunt open-circuited resonators that are quarter-wavelength long and straight with connecting lines that are also quarter-wavelength long. These BSFs normally have the narrow stopband. As wide stopband response is required in BSFs, the techniques of photonic band gap (PBG) periodic structures [2] and the defected ground plane (DGS) structures [3] are alternative solutions.

The anti-coupled lines with short circuits at one end reveal characteristics of multiple transmission zeros. Therefore, it is viewed as one kind of frequency-selecting coupling structure (FSCS) in this work. In this work, combining one shunt series open-circuited resonator that is quarter-wavelength long and straight with one section of quarter-wavelength FSCS can induce three transmissions zeros in the stopband. Herein, the quarter-wavelength open-circuited resonator is used instead of the half-wavelength short-circuited resonator since bandpass filter is not the main subject of this work. For the purpose of further miniaturization, other arbitrary open-circuited stubs that are electrically quarter-wavelength long can be adopted as the series resonators. With the aid of extra transmission zeros, the low-order BSF, which normally has a smaller circuit size and a lower insertion loss, successfully achieve the wide stopband.

Manuscript received November 19, 2004; revised January 31, 2005. The review of this letter was arranged by Associate Edior M. Mrozowski.

The authors are with National Chiao-Tung University, Hsinchu 300, Taiwan, R.O.C. (e-mail: yoho.cm90g@nctu.edu.tw).

Digital Object Identifier 10.1109/LMWC.2005.851572

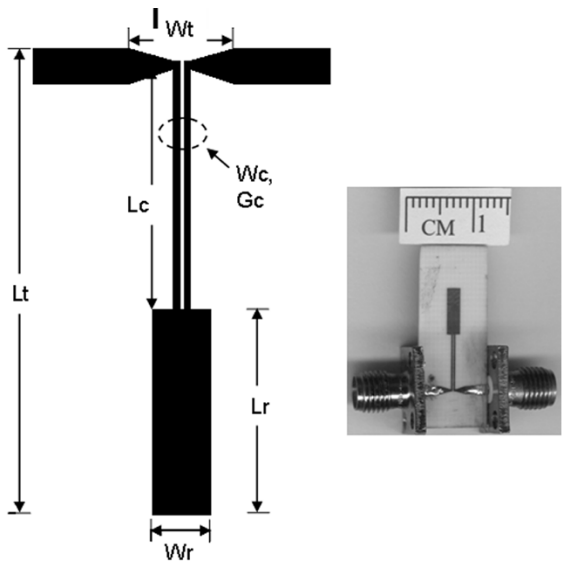

Fig. 1. Photograph of the proposed BSF.

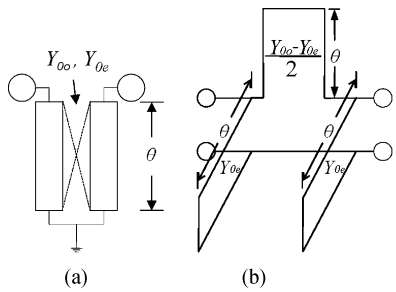

Fig. 2. Schematic of one FSCS and its equivalent circuit based on TEM-mode.

II. Analysis of Novel BSF With Integrated Frequency-Selecting Coupling Structure

As shown in Fig. 1, the novel BSF structure composed of single open-circuited quarter-wavelength resonator and one section of quarter-wavelength FSCS was not reported in the past. In Fig. 1, the shunt open-circuited resonator that is quarter-wavelength long at the center frequency of stopband plays the role of series L–C resonator.

A. Frequency-Selecting Coupling Structure

As shown in Fig. 2, the schematic of lossless FSCS and its equivalent circuit [4] that is based on TEM mode can be ana-

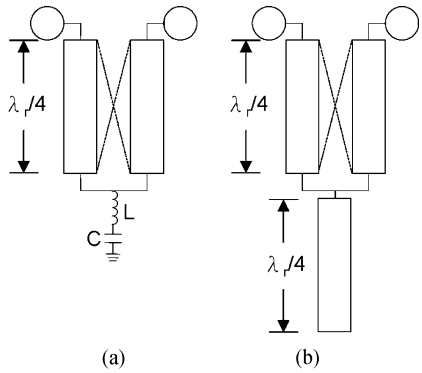

Fig. 3. (a) FSCS with series L–C resonator. (b) FSCS with open-circuited quarter-wavelength resonator.

lyzed by the classical method of even- and odd-mode excitation. The transmission coefficient S_{21} [1] is given by

$$S_{21} = \frac{\Gamma_e - \Gamma_o}{2} = \frac{Y_{\rm ino}}{Y_0 + Y_{\rm ino}} - \frac{Y_{\rm ine}}{Y_0 + Y_{\rm ine}} \tag{1}$$

where $\Gamma_{\rm e}$ and $\Gamma_{\rm o}$ are the reflection coefficients, $Y_{\rm ine}$ and $Y_{\rm ino}$ are the input admittances for even- and odd-mode excitations, and Y_0 is the system admittance. The transmission-zero condition of FSCS is

$$Y_{0o}\cot\theta = Y_{0e}\cot\theta \tag{2}$$

where Y_{0e} and Y_{0o} are the even- and odd-mode characteristic admittances.

From Fig. 2(a) and (2), one transmission zero is induced when $\theta = 90^\circ$ at f_r where f_r is the frequency at which the FSCS is quarter-wavelength long. Unfortunately, in microstrip structure, because the even-mode phase velocity of the microstrip coupled lines is always slower than that of the odd-mode one, the even-mode electrical length θ_e is always larger than odd-mode electrical length θ_o for all frequencies. Therefore, this transmission zero is located at the frequency upper f_r. In this work, adjusting the coupling length slightly longer than quarter-wavelength can move the transmission zero toward f_r and solve this problem.

B. One BSF Unit

In Fig. 3(b), the FSCS and shunt open-circuited resonator have the electrical length of $\pi/2$ and $Y_{\rm r}$ is the characteristic admittance of resonator. It can be observed that both load-impedance functions (3) and (4) from Fig. 3(a) and (b), respectively, have the same characteristics in the vicinity of $\omega = \omega_0$. These equations are listed as

$$Z_L = j\omega_0 L\left(\frac{\omega}{\omega_0} - \frac{\omega_0}{\omega}\right) \approx \pm j2L\Delta\omega \tag{3}$$

$$Z_L = \frac{jZ_r\pi}{4}\left(\frac{\omega}{\omega_0} - \frac{\omega_0}{\omega}\right) \approx \pm\frac{jZ_r\pi}{2}\frac{\Delta\omega}{\omega_0} \tag{4}$$

where $\omega = \omega_0 \pm \Delta\omega$.

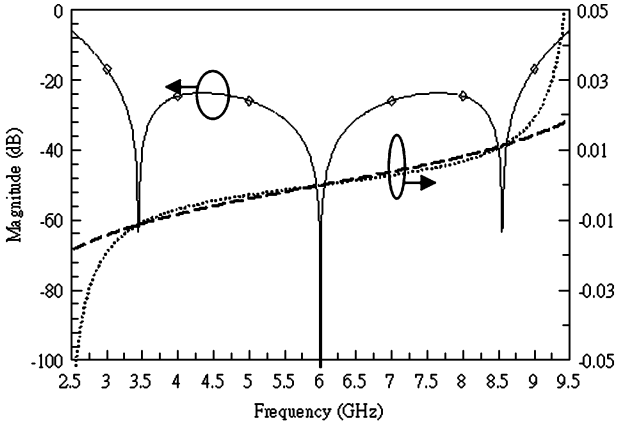

Fig. 4. Calculated TEM-mode performance of one BSF cell. —$\mathrm{DB}[S_{21}]$; —$\mathrm{Im}[Y_{\rm ino}]$; $\cdots\cdots$ $\mathrm{Im}[Y_{\rm ine}]$.

Herein, the BSF structure in Fig. 3(b) is also analyzed by the method of even- and odd-mode excitations. The even- and odd-mode input admittances of one BSF unit are given as

$$Y_{\rm ine} = Y_{0e}\frac{Y_{\rm Le} + jY_{0e}\tan\theta}{Y_{0e} + jY_{\rm Le}\tan\theta} \tag{5a}$$

$$Y_{\rm ino} = -jY_{0o}\cot\theta \tag{5b}$$

where

$$Y_{\rm Le} = 1/Z_{\rm Le} = 1/(2Z_L) = \frac{jY_r\tan\theta}{2}. \tag{5c}$$

The condition of transmission zero ($S_{21} = 0$) is $Y_{\rm ine} = Y_{\rm ino}$. It indicates that $\mathrm{Im}[Y_{\rm ine}]$ is equal to $\mathrm{Im}[Y_{\rm ino}]$. The imaginary parts of even- and odd-mode input admittances are given by

$$\mathrm{Im}[Y_{\rm ine}] = -Y_{0e}\cot\theta\cdot a \tag{6a}$$

$$\mathrm{Im}[Y_{\rm ino}] = -Y_{0o}\cot\theta \tag{6b}$$

where

$$a = \frac{1 - (Y_{0e}/Y_{\rm Le})^2}{1 + (\cot\theta\cdot Y_{0e}/Y_{\rm Le})^2} = \frac{1 + (2\cdot\cot\theta\cdot Y_{0e}/Y_r)^2}{1 - (2\cdot\cot^2\theta\cdot Y_{0e}/Y_r)^2}.$$

Because $Y_{0\rm o}$ and a are larger than $Y_{0\rm e}$ and 1, respectively, the created transmission zeros are at the frequencies when $\theta = \pi/2$ and $\theta = (\pi/2) \pm \Delta\theta$ where $\Delta\theta$ is positive. By using (6) to plot Fig. 4, the intersection points show the locations of the transmission zeros. Thus, the wide stopband can be formed as shown in Fig. 4. For this TEM-mode BSF, we adopt $Z_{0e} = 147\Omega$, $Z_{0o} = 70\Omega$, and $Z_r = 35\Omega$.

In the following, the equations from (4)–(6) for small $\Delta\omega$ are given as

$$\frac{1 + \left(\frac{\pi}{2}\frac{Y_{0e}}{Y_r}\frac{\Delta f}{f_r}\right)^2}{1 - \left(\frac{Y_{0e}}{Y_r}\right)^2\left(\frac{\pi}{2}\frac{\Delta f}{f_r}\right)^4} = \frac{Y_{0o}}{Y_{0e}} > 1 \tag{7}$$

$$\frac{\Delta f}{f_r} \propto \frac{Y_r}{Y_{0e}}\sqrt{\frac{Y_{0o}}{Y_{0e}} - 1}. \tag{8}$$

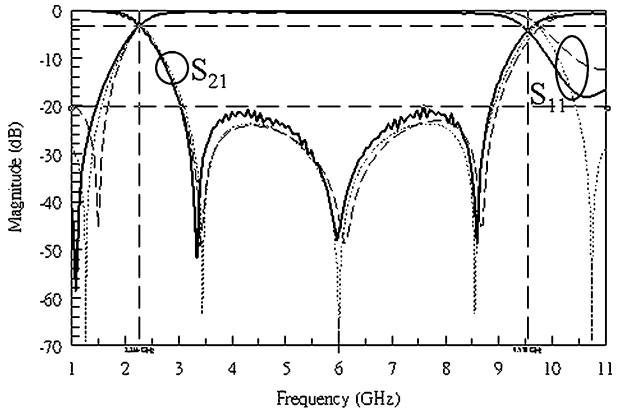

Fig. 5. Calculated TEM-mode simulated EM, and measured performance of one BSF cell. —Measured; —Simulated EM; · · ·Calculated TEM-mode.

III. Band-Stop Filters With Wide Stopband

A planar and wide stopband BSF in Fig. 1 is fabricated by following the procedures listed as follows:

1) decides the center frequency of the fundamental stopband;
2) initially designs the quarter-wavelength resonator and FSCS in the homogeneous medium for satisfying the requirements;
3) chooses appropriate dimensions of quarter-wavelength resonator and FSCS in an inhomogeneous medium;
4) fine adjusts the dimensions of quarter-wavelength resonator and FSCS to make agreement between the simulated results in homogeneous medium and those in inhomogeneous medium.

Adjusting the coupling gap of FSCS can control bandwidth of stopband. A smaller gap results in a stronger coupling, thus wider bandwidth is achieved, as indicated in (8). Moreover, a distributed-line resonator of higher characteristic admittance in Fig. 1 also broadens the stopband.

IV. Simulated and Experimental Results

To confirm the idea of the novel BSF structure, one-section BSF was fabricated as shown in Fig. 1 on the RO4003 substrate with a relative permittivity of ε_r =3.38, thickness of h =0.508 mm, and loss tangent of 0.0027. This BSF is connected to the 50-Ω input and output transmission line. Its circuit size without the SMA connectors and 50-Ω transmission lines is 3.6×15.5 mm^2. The parameters of the designed BSF are Lr =6.8 mm, Wr =2 mm, Lc =8 mm, Wc =0.2 mm, and Gc =0.15 mm. These values are adjusted to fit the performance of TEM-mode BSF.

Fig. 5 shows the simulated and experimental results. It indicates that there is good agreement between simulated and measured responses. The simulation is performed with the aid of commercial circuit and Sonnet Software full-wave simulators [5]. The center frequency f_r and 3-dB fractional bandwidth Δ of the proposed BSF is close to 6 GHz and 120%, respectively. An Agilent 8720ES network analyzer is used to perform the measurement.

V. Conclusion

In this work, we have addressed the design and performance of the proposed BSF with wide stopband. It is noted that the advantage of the proposed BSF over the conventional broadband BSF is its easiest fabrication and compact size. The improvement of the stopband of BSF in this work is because of inducing extra transmission zeros in the stopband by means of combining one shunt open-circuited quarter-wavelength resonator with one section of quarter-wavelength FSCS. Therefore, a novel BSF that balances lower-order resonators, good stopband performance, simple structure, and uncomplicated design procedure was successfully implemented.

Acknowledgment

The authors would like to thank reviewers, for suggesting several improvements in this letter's manuscript, and Dr. Chang, for his valuable suggestions and encouragement.

References

[1] J. S. Hong and M. J. Lancaster, *Microstrip Filters for RF/Microwave Applications*. New York: Wiley, 2001.
[2] C. Y. Hang, W. R. Deal, T. Qian, and T. Itoh, "High efficiency transmitter front-ends integrated with planar an PBG," in *Asia-Pacific Microwave Conf. Dig.*, Dec. 2000, pp. 888–894.
[3] J.-Y. Kim and H.-Y. Lee, "Wideband and compact bandstop filter structure using double-plane superposition," *IEEE Microw. Wireless Compon. Lett*, vol. 13, no. 7, pp. 279–280, Jul. 2003.
[4] G. L. Matthaei, L. Young, and E. M. T. Jones, *Microwave Filters, Impedance-Matching Networks, and Coupling Structures*. Norwood, MA: Artech House, 1980.
[5] *Sonnet Std. 6.0a*, Sonnet Software, Inc., 2005.